Perimeter Effects on Ring Currents in Polycyclic Aromatic Hydrocarbons: Circumcoronene and Two Hexabenzocoronenes

ARTICLE *in* CHEMISTRY - A EUROPEAN JOURNAL · JULY 2003

Impact Factor: 5.73 · DOI: 10.1002/chem.200204183 · Source: OAI

Perimeter Effects on Ring Currents in Polycyclic Aromatic Hydrocarbons: Circumcoronene and Two Hexabenzocoronenes

Alessandro Soncini,[a] Erich Steiner,[a] Patrick W. Fowler,*[a] Remco W. A. Havenith,[a, b] and Leonardus W. Jenneskens*[b]

Abstract: Current-density maps are calculated at an ab initio level for the three symmetrical polycyclic aromatic hydrocarbons, circumcoronene [**1** (D_{6h})], hexabenzo[*bc*,*ef*,*hi*,*kl*,*no*,*qr*]coronene [**2a** (D_{6h}) and **2b** (D_{3d})], and hexabenzo[*a*,*d*,*g*,*j*,*m*,*p*]coronene [**3a** (D_{6h}), **3b** (D_6) and **3c** (D_{3d})], all of which can be formally derived by annelation of benzene rings to a coronene core. Whilst **1** is planar, **2** has a non-planar minimum that is effectively isoenergetic with its planar form, and **3** has a well defined non-planar structure. The shape of the molecular boundary rather than the planarity of the molecule plays the critical rôle in the character of the predicted currents. Formal deletion of outer hexagons from circumcoronene (**1**) in two different ways produces either hexabenzocoronene **2** with a prediction of *disjoint* local benzenoid diatropic currents linked by a global perimeter, or **3** with a *giant* diatropic perimeter current enclosing a weak paramagnetic circulation on the central hexagon. The current density map of **1** is effectively a superposition of those of **2** and **3**. Its strong diatropic perimeter current subsumes the six weaker diatropic benzenoid circulations evident in **2**, and bifurcates in the six outer benzenoid rings that form the corners of the giant hexagon; its benzene "hub" sustains a diatropic current, as would be expected from the partial cancellation of the strong diatropic hub current of **2** by the weaker paratropic hub current of **3**. The relationship between the three molecules is rationalised by considering orbital contributions to their current density maps.

Keywords: arenes · aromaticity · NMR spectroscopy · ring currents

Introduction

Large polycyclic aromatic hydrocarbons (PAHs) are ubiquitous combustion products. They have been implicated as carcinogens and play a rôle in graphitisation of organic materials.[1] In addition, they are of interest as molecular analogues of graphite,[2] as candidates for interstellar species[3] and as building blocks of functional materials for device applications.[2, 4] Synthetic routes to PAHs are available,[5] though the size and poor solubility of the bare, unfunctionalised molecules hamper their structural characterisation and the elucidation of their physicochemical properties.[2, 6] This is unfortunate, as both molecular size and boundary shape influence electronic structures, energetics and reactivity,[7] and a detailed knowledge of all these features would therefore be necessary for the tuning of molecular properties towards specific applications.

One way to assess perimeter effects in these large PAH systems is through calculation of magnetic properties. In the present paper we use the CTOCD-DZ distributed-origin, ab initio method[8] (see Computational Methods for details) to visualise the current density induced by a perpendicular external magnetic field in the planar forms of circumcoronene (**1**, $C_{54}H_{18}$) and two derivatives that can be formally derived from it by removal of boundary hexagons, planar hexabenzo[*bc*,*ef*,*hi*,*kl*,*no*,*qr*]coronene (**2a**, $C_{42}H_{18}$)[9] and hexabenzo[*a*,*d*,*g*,*j*,*m*,*p*]coronene (**3a**, $C_{48}H_{24}$) (Scheme 1).[10] Scheme 1 illustrates one Kekulé structure for each system, out of the 980, 250 and 432 possibilities for **1**, **2** and **3**, respectively.[11] Current density maps give a direct description of *global* and *local* ring currents in polycyclic π-conjugated systems and, by integration yield the properties such as magnetisability (susceptibility anisotropy and exaltation), ^{1}H NMR chemical shifts and nucleus independent chemical shifts (NICS),[12] that are typically used to characterise global and local aromaticity in polycyclic systems.

[a] Prof. Dr. P. W. Fowler, A. Soncini, Dr. E. Steiner, Dr. R. W. A. Havenith
School of Chemistry, University of Exeter
Stocker Road, Exeter EX4 4QD (UK)
Fax: (+44) 1392-263434
E-mail: p.w.fowler@exeter.ac.uk

[b] Prof. Dr. L. W. Jenneskens, Dr. R. W. A. Havenith
Debye Institute, Department of Physical Organic Chemistry
Utrecht University, Padualaan 8, 3584 CH Utrecht (The Netherlands)
Fax: (+31) 30-2534533
E-mail: jennesk@chem.uu.nl

Supporting information for this article is available on the WWW under http://www.chemeurj.org or from the author. Total energies (E_{tot} in E_h; RHF/6-31G**) and cartesian coordinates (RHF/6-31G** in a.u.) of **1** (D_{6h}), **2a** (D_{6h}), **2b** (D_{3d}), **3a** (D_{6h}), **3b** (D_6) and **3c** (D_{3d}).

DOI: 10.1002/chem.200204183

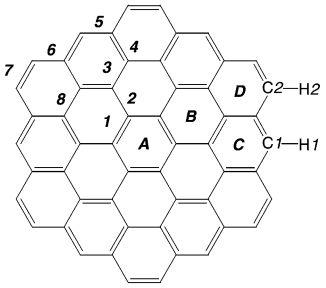

1

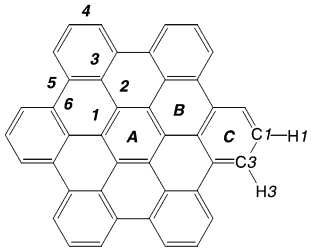

2a–c

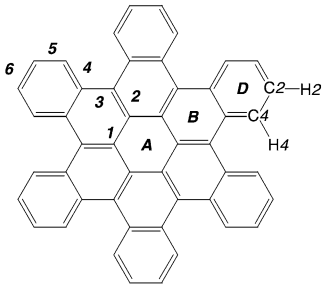

3a–c

Scheme 1. Schematic representation of circumcoronene (**1**) and the hexabenzocoronenes **2a**, **b** and **3a–c**.

Computational Methods

The geometries of all three molecules were optimized at the RHF/6-31G** level with the CADPAC[13] and GAUSSIAN98 packages.[14] Appropriate symmetry constraints were applied (see Results and discussion section and Supporting Information). The computation of the current density maps of **1**, **2a–b** and **3a–c** was performed using the DZ (diamagnetic zero) variant of the distributed-origin CTOCD (continuous transformation of origin of current density) method (CTOCD-DZ),[8] as implemented in SYSMO,[15] using a 6-31G** basis set. The maps show the π current density induced by unit magnetic field acting at right angles to the molecular plane and are, in the case of the planar D_{6h} structures **1**, **2a** and **3a**, plotted in the plane 1 a_0 above that of the nuclei. Current density maps at this height above the molecular plane remain essentially unchanged when larger basis sets are used.[16] The contours show the modulus of current density with values 0.001×4^n a.u. for $n = 0,1,2,\ldots$ and the vectors represent in-plane projections of current. For the non-planar structure **2b** the map was plotted in the plane 1 a_0 above the median plane of the molecule, and for **3c** special local sectional plots were made (see Results and Discussion section). In all maps the diamagnetic circulation is shown anti-clockwise, the paramagnetic circulation clockwise. Orbital contributions[17] were also mapped in several cases (see Results and Discussion section). Integrated magnetic properties such as the magnetisability and shieldings at nuclei (e.g. ^{1}H NMR chemical shifts) and ring centres (e.g. NICS values) are computed in the PZ2 (paramagnetic zero) variant of the CTOCD method (CTOCD-PZ2),[18] which is more accurate for this purpose.[19]

Results and Discussion

Geometries of 1, 2a–b and 3a–c: Whereas a planar structure (D_{6h} symmetry) was found for **1**, in the case of **2** and **3** the structures with D_{6h} symmetry, **2a** and **3a**, were higher order saddle points [$E_{tot.}$(RHF/6-31G**): **1** (D_{6h}) −2055.7817, **2a** (D_{6h}) −1601.2048, and **3a** (D_{6h}) −1831.5437 E_h]. Hessian calculations gave respectively 3 and 10 imaginary vibrational frequencies for **2a** and **3a** [**2a**; 23*i*, 18*i* (doubly degenerate) cm^{-1}) and **3a**; 841*i*, 829*i* (doubly degenerate), 803*i* (doubly degenerate), 789*i*, 178*i*, 132*i* (doubly degenerate), 10*i*, cm^{-1})]. When the D_{6h} symmetry constraint was relaxed, true minima with non-planar geometries were located for **2** [**2b** (D_{3d})] and **3** [**3b** (D_6) and **3c** (D_{3d})] [$E_{tot.}$(RHF/6-31G**): **2b** −1601.2049, **3b** −1831.7726 and **3c** −1831.8331 E_h (see also Supporting Information)]. Scheme 2 shows the three-dimensional structures of the three non-planar minima **2b**, **3b** and **3c**.

2b

3b

3c

Scheme 2. RHF/6–31G** structures of **2b**, **3b** and **3c** (see text).

Thus, the relaxation to lower symmetry gave for **2** a non-planar structure with D_{3d} symmetry that is essentially isoenergetic (ΔE_{tot} 0.3 kJ mol^{-1}) with planar **2a**. In line with the small imaginary frequencies found for **2a**, hexabenzocoronene **2** has apparently a very shallow potential-energy surface connecting planar and non-planar structures.

For hexabenzocoronene **3**, two well defined non-planar minima were located, one with a propeller shape [**3b** (D_6)] and one with a double-trefoil shape [**3c** (D_{3d})], which are respectively, 600 and 760 kJ mol^{-1} more stable than their planar analogue **3a** (D_{6h}). The large energy difference between **3a** and **3b, c** is attributable to the six-fold occurrence of steric congestion between the two non-bonded bay-region hydrogen atoms. The H*4*—H*4′* distance relaxes from 1.235 Å in **3a**, to 2.049 Å in **3b**, and 2.150 Å in **3c** (see Scheme 1). Similar steric interactions are responsible for the non-planarity of benz[*c*]phenanthrene[20] for which the corresponding non-bonded distance is 1.573 Å in the planar-constrained C_{2v} geometry and 1.978 Å in the C_2 optimal structure [RHF/6-31G**: $\Delta E_{tot.} = E_{tot.}(C_{2v}) - E_{tot.}(C_2) = 20$ kJ mol^{-1}].

In Table 1 the symmetry-independent bond lengths of **1**, **2a–b**, **3a–c** are reported (see also Scheme 1). A comparison

Table 1. Computed symmetry independent bond lengths [Å] of **1**, **2a**, **b** and **3a–c**.

	Compounds					
Bond length [a]	**1** (D_{6h})	**2a** (D_{6h})	**2b** (D_{3d})[b]	**3a** (D_{6h})	**3b** (D_6)[b]	**3c** (D_{3d})[b]
1	1.405	1.409/1.4173[c]	1.407	1.497	1.451	1.444
2	1.433	1.455/1.4467[c]	1.454	1.411	1.388	1.378
3	1.405	1.409/1.4175[c]	1.408	1.482	1.451	1.452
4	1.412	1.376/1.3758[c]	1.376	1.430	1.423	1.413
5	1.390	1.391/1.3990[c]	1.391	1.353	1.360	1.365
6	1.445	1.467/1.4583[c]	1.467	1.373	1.404	1.399
7	1.340			1.406	1.397	1.405
8	1.431					

[a] See Scheme 1. [b] Deviation from planarity of these molecules can be expressed by the height from the median plane of the perimeter carbon atoms and their attached hydrogens (**2b**: C*1* 0.20 and H*1* 0.29 Å, and, C*3* 0.14 and H*3* 0.20 Å, **3b**: C*2* 0.29 and H*2* 0.56 Å, and, C*4* 0.46 and H*4* 0.36 Å, **3c**: C*2* 1.47 and H*2* 1.90 Å, and, C*4* 0.96 and H*4* 1.05 Å). [c] Symmetry-averaged bond lengths from the single crystal X-ray structure of **2a**, which was found to be planar.[21]

of computed and symmetry-averaged, single-crystal X-ray structural data[21] for **2a** shows satisfactory agreement.

Current density maps: Maps for induced current density for **1**, **2a** and **3a**, are shown in Figure 1. The 1 a_0 plotting plane is close to the maximum in both π-charge and π-current density in hydrocarbons, and at this height the flow is essentially parallel to the molecular plane[22] so that no significant error is introduced by neglecting the component of current density parallel to the inducing field. We begin by discussing the π-only and total (σ + π) maps for the planar forms of the hexabenzocoronenes, **2a** and **3a**, before relating them to those for the formal parent molecule **1**.

The π-only current density map of molecule **2a** (Figure 1c) shows seven *disjoint* diamagnetic (diatropic) circulations corresponding to the benzene rings that carry Clar sextets[23] in the classical picture of this totally resonant PAH. The six outer benzenoid circulations are linked by a global ring current around the perimeter of the molecule.

In a graph-theoretical approximation, current flow along the six bonds that radiate from the central hexagon is rigorously forbidden for **2a** and **3a** by the magnetic point group symmetry,[24] and in the ab initio π-

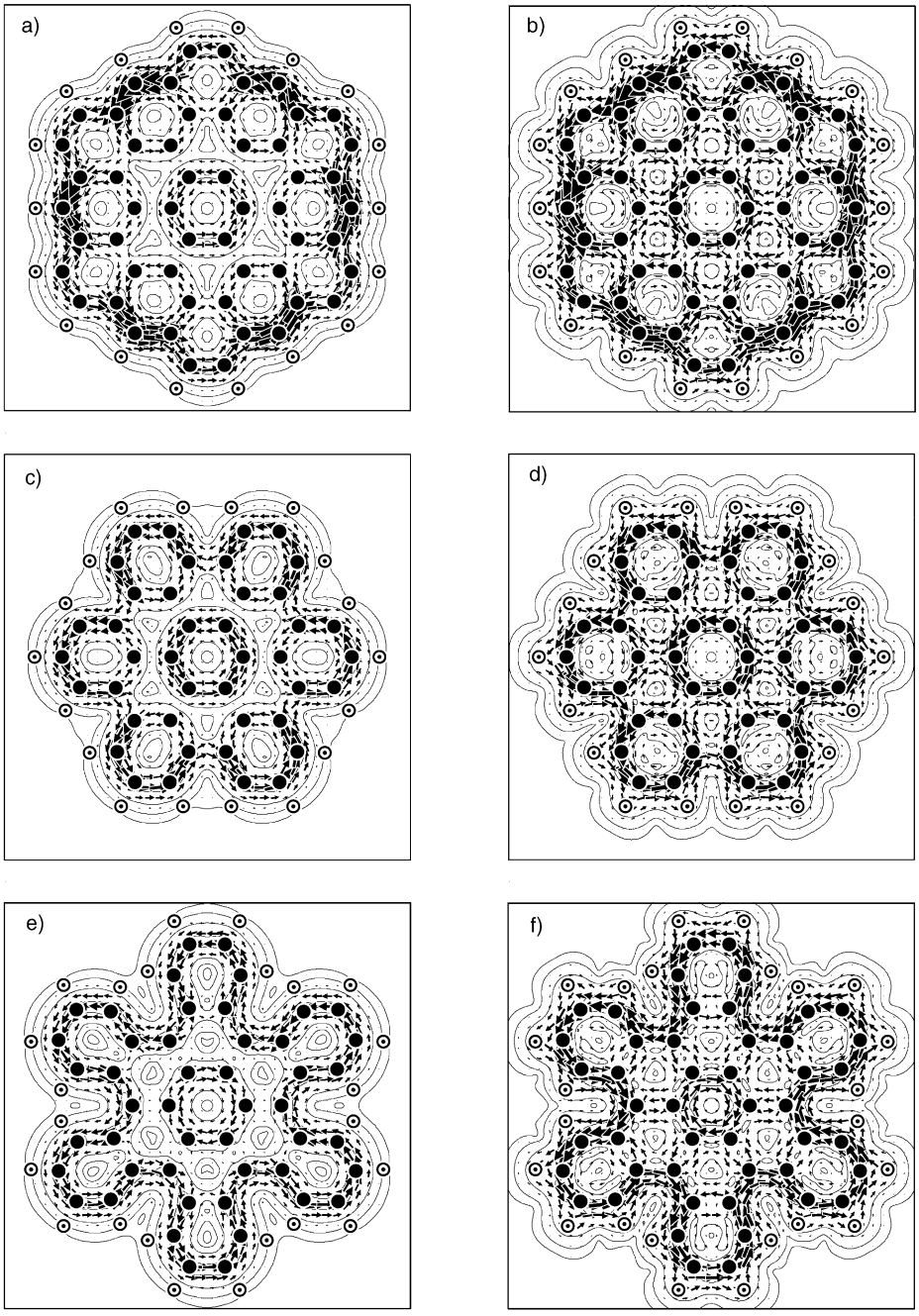

Figure 1. Computed current density maps for planar **1**, **2a** and **3a**; (a), (c), (e) π-only and (b), (d), (f) total (σ + π) for **1**, **2** and **3a**, respectively (carbon ● and hydrogen ⊙).

only maps for all three planar and planarised species it can be seen that these bonds remain devoid of significant circulation.

When σ electrons are taken into account, the currents in **2a** are intensified, enhancing the pattern of disjoint benzenoid currents [total (σ + π) map, Figure 1d]. The σ electrons also introduce paramagnetic vortices at the hexagon centres as the usual consequence of the presence of localised σ bond circulations; these vortices have maximum strength in the molecular plane and in Figure 1 they are seen most clearly over the six *non*-Clar rings.

The current density maps of planar **3a** shows a distinctly different overall pattern. The most notable feature of the π-only map (Figure 1e) is the single, giant, perimeter ring current that follows the corrugations of the boundary. This strong diamagnetic current is opposed by a disjoint, and weaker paramagnetic (paratropic) circulation on the central hexagon. The co-existence of counter-rotating rim and hub currents is reminiscent of coronene itself.[25] Inclusion of σ electrons again intensifies the currents, but without changing the pattern.

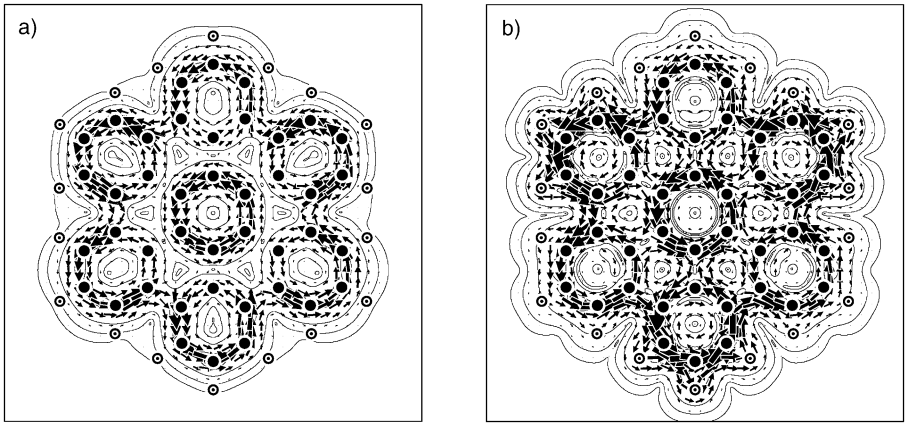

Figure 2. Computed current density maps for non-planar **2b**; a) "π-only" and b) total ("σ + π") (carbon ● and hydrogen ⊙).

Influence of non-planarity: In Figure 2a, b the "π-only" and total current-density maps for non-planar **2b** are shown. Despite the loss of exact σ–π separability in the non-planar structure, the orbitals derived by descent in symmetry from the original π-set of **2a** retain their essential character and give rise to the same Clar sextet pattern of current density in the map (Figure 2a). The maps of total ("σ + π") current density for **2a** and **2b** are also closely similar (Figure 2b); the currents in the outer hexagons show some alternation in strength on the perimeter between successive rings lying above and below the median plane but from this minor symmetry breaking effect the patterns are hardly affected by the loss of planarity.

Non-planarity might be expected to play a more significant role in the current distribution for the chiral propellor-shaped D_6 symmetric **3b**. The deviation from planarity and from formal σ–π separability is greater for this molecule than for **2b**, but as Figure 3 shows, the "π-derived" orbitals still lead to a perimeter circulation that is recognisably the same as in the planar form **3a**. The geometric corrugation leads to undulation in the current vectors but there is still a single diatropic global circulation around the perimeter and a weaker paratropic central current as in **3a**. This similarity between **3a** and **3b** also extends to the maps of total current density.

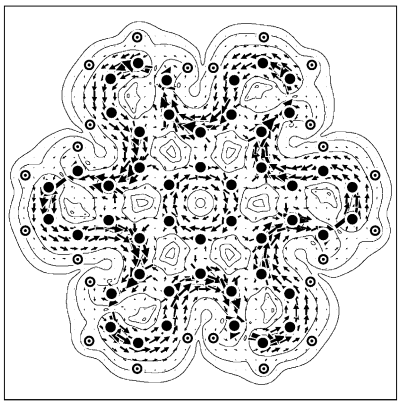

Figure 3. Computed "π-only" current density maps for non-planar **3b** (carbon ● and hydrogen ⊙).

For the stable form of **3**, the D_{3d} structure **3c**, the deviation from planarity is larger and the double-trefoil structure consists of a planar central region with six locally planar hexagonal petals. To avoid complications arising from the strong undulations in the current density in this non-planar conformation, sectional maps of the central and petal regions are shown separately in Figure 4. Figure 4a shows the total

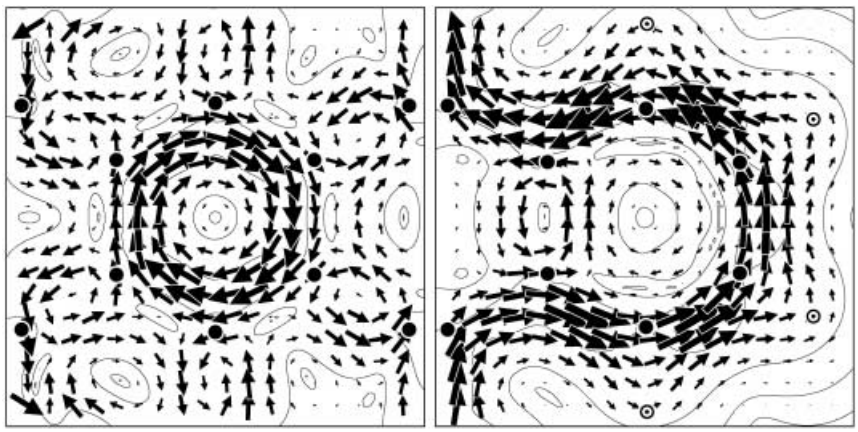

Figure 4. Computed current density maps for non-planar **3c**. A composite map shows (left) the total current density over the central region and the total current density over an outlying hexagon (right), in each case induced by a magnetic field perpendicular to the respective median plane. In each half of the picture, the plotting plane lies at a distance of 1 a_0 from the median plane. The pair of common carbon centres show how the two regions join together (carbon ● and hydrogen ⊙).

current density induced in a plane 1 a_0 above the central hexagon of 3c by a magnetic field along the C_3 principal axis; Figure 4b shows the total current density induced in a plane 1 a_0 above/below the local median plane of one of the six outer hexagons by a magnetic perpendicular to this plane. As can be seen from Figure 4b, the non-planar structure **3c** retains the central paratropic circulation and the strong diatropic perimeter circulation that loops through the outer hexagons. In all essentials **3c** has the same global pattern of circulations as the planar form **3a** (see also Figure 1).

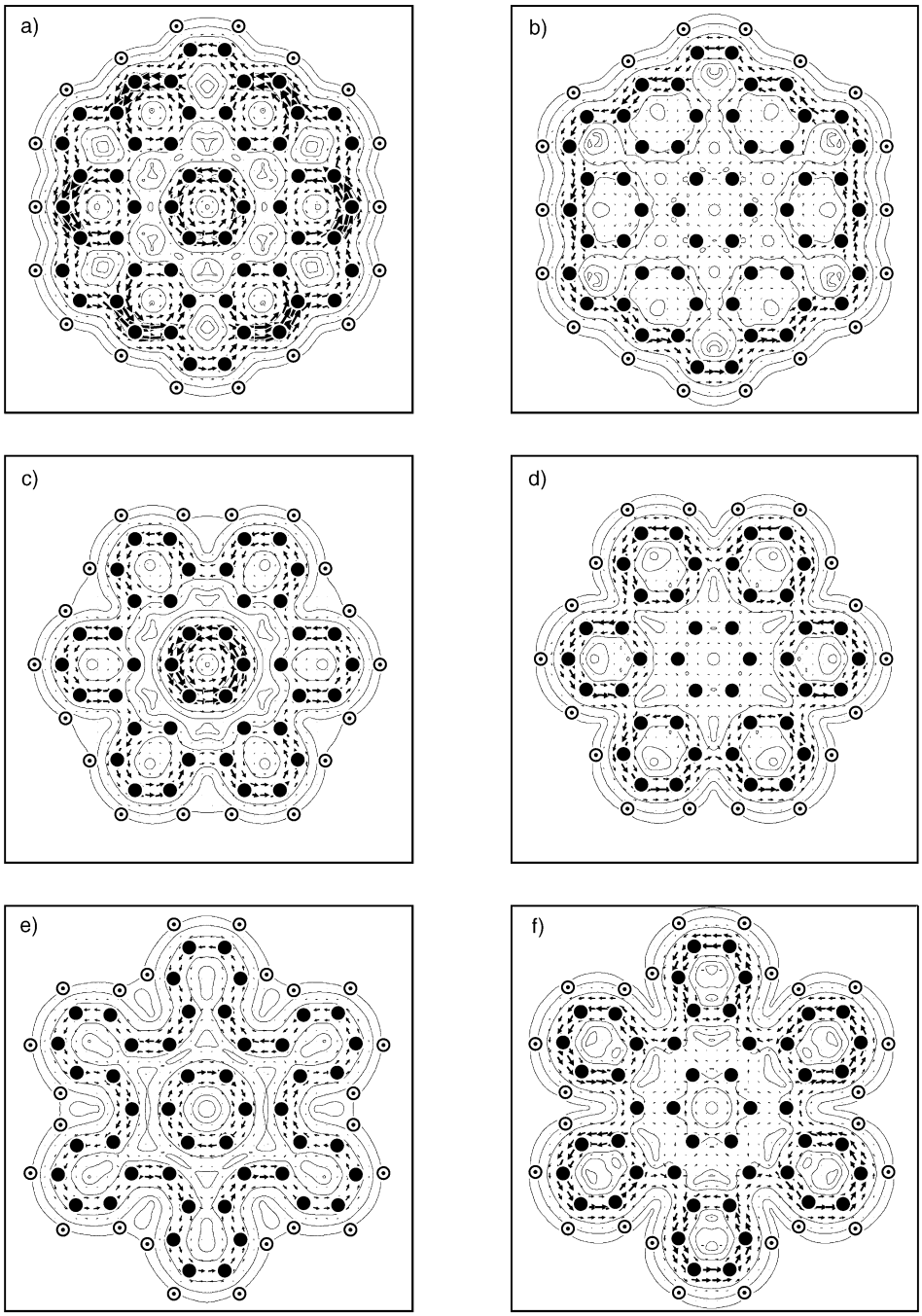

Figure 5. Contributions to the π current density maps for **1**, **2a**, and **3a**; (a), (c), (e) from the four π electrons in the doubly degenerate HOMO (**1** e_{1g}, **2a** e_{1g}, **3a** e_{2u}) and (b), (d), (f) from all the remaining π electrons (carbon ● and hydrogen ⊙).

Orbital analysis: How do these results relate to the maps for the parent circumcoronene (**1**)? As Figure 1 shows, the π map for **1** is essentially a superposition of the corresponding maps for **2a** and **3a**, with some enhancement of the diamagnetic ring current around the perimeter. The global circulation now subsumes the six weaker circulations in the "Clar" hexagons that were evident in **2**, and also bifurcates across the six outer rings that form the "corners" of the giant hexagon. The central ring of **1** is diamagnetic, as would be expected from the partial cancellation of the strong central current of **2a** by the weaker hub current of **3a**.

A more informative picture of the relationship between the three molecules is derived by considering orbital contributions to their current density maps. (For simplicity we concentrate on the planar forms of the three molecules.) The CTOCD-DZ (*ipsocentric*) formulation of orbital current density[17, 26] has been shown to provide a succinct and physically based analysis of these contributions. In this approach, for example, the bulk of the π current in the classical $(4n+2)$ mono-cycles comes from the four π electrons in the highest occupied molecular orbitals (HOMO)[26] and, more generally,[17] the current density is dominated by contributions from electrons in a small number of orbitals close to the molecular Fermi level. The same partition scheme can be applied here. The density maps shown in Figure 5 are the contributions to the total π-only maps (of Figure 1) from (on the left) the four electrons in the doubly-degenerate HOMO of each planar system and from (on the right) all the remaining π electrons (of which there are 50 in **1**, 38 in **2**, and, 44 in **3**). In all three molecules the π systems *minus* the HOMO electrons provides a uniform diatropic perimeter circulation (of strength about 2/3 of the benzene value); in **1a** this is effectively confined to the perimeter, in **2a** and **3a** it consists of benzenoid circulations in the six protruding hexagons (Figure 5b, d and f). It is the HOMO contribution in each case that gives the π map its characteristic central

feature, though it also modifies the perimeter circulation. In the three molecules, the HOMO electrons are responsible for about half of the perimeter current and almost all of the central hub current (Figure 5a, c and e). A further breakdown of the non-HOMO contribution shows that the perimeter current densities are in fact associated with a group of only about seven orbitals lying close to the HOMO. This concentration of the magnetic response into contributions from only the higher lying occupied orbitals is a characteristic feature of the ipsocentric method.[17, 26] It suggests that the effective number of electrons determining properties such as magnetisability will grow more slowly than the total number of π electrons in these extended conjugated systems.

The basic patterns seen in the ab initio maps for **1**–**3** are manifestations of the different topologies of the molecules. Indeed, a purely graph-theoretical model such as the π-only Hückel–London theory[27] is capable of reproducing the main features of the π-current density. This model, which has only a small number of independent bond currents (four for **1**, three each for **2a** and **3a**, Figure 6) correctly predicts the sense of circulation in each ring, the differing global behaviour of **1**, **2** and **3** and the overall patterns and approximate relative magnitudes of the currents.

Global and local magnetic properties: Global molecular magnetic properties also bear out the qualitative features displayed by the current density maps. In particular, the picture of **1** as a combination of the features of **2** and **3** is supported by the computed magnetisability anisotropy, $\Delta\xi$ of **1** (−314 a.u.), which is almost exactly the sum of those for **2a** (−148 a.u.) and **3a** (−156 a.u.). Benzene and coronene calculated at the same level of theory have $\Delta\xi$ values of −16.5 and −102 a.u., respectively.[25]

The detailed maps of current density complement various local measures of aromaticity based on ring current, such as the estimates available from calculations of NICS values.[12] In Table 2 are shown magnetic shieldings at ring centres,

Table 2. Magnetic shielding tensors at centres of rings of **1**, **2a, b** and **3a**–**c**; σ(out), σ(in) and σ(av) [ppm] are the *out-of-plane* component, the mean in-plane component and the mean, respectively. The NICS[12] value in the ring centre is obtained by change of sign of σ(av). For the non-planar compounds, only the *isotropic* values σ(av) are tabulated.

Compound[a]	σ	*A*	*B*	*C*	*D*
1 (D_{6h})	σ(out)	26.3	−11.8	29.7	−4.9
	σ(in)	14.8	14.9	14.5	15.1
	σ(av)	18.6	6.0	19.5	8.4
2a (D_{6h})	σ(out)	22.9	−24.3	13.1	
	σ(in)	14.9	15.1	13.5	
	σ(av)	17.6	1.9	13.4	
2b (D_{3d})	σ(av)	17.6	2.0	13.5	
3a (D_{6h})	σ(out)	−38.3	−3.1		12.8
	σ(in)	15.7	14.9		13.6
	σ(av)	−2.3	8.9		13.3
3b (D_6)	σ(av)	−3.0	7.8		11.5
3c (D_{3d})	σ(av)	−1.9	7.6		13.1

[a] See Scheme 1.

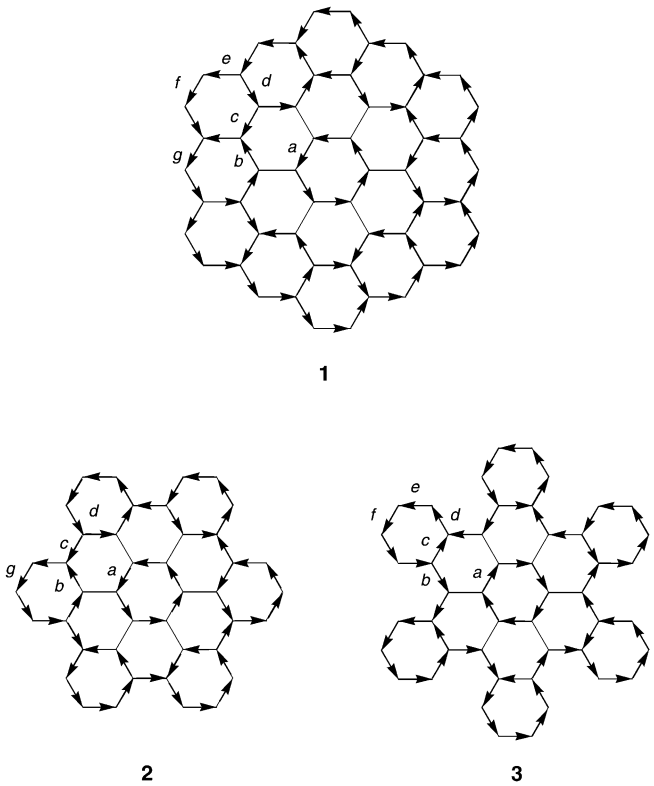

Figure 6. Induced bond currents in the π-only Hückel–London model of **1**, **2** and **3**. The molecules are fixed in the plane with all bond lengths set to 1.40 Å, and all the resonance integrals are set to the benzene β value; **1**, $a = 0.661$, $b = 0.355$, $c = 0.309$ and $e = 1.487$, with $d = b + c$, $f = e$ and $g = d + f$, **2**, $a = 0.963$, $b = 0.491$ and $c = 0.849$, $d = b + c$, $g = d$, and, **3**, $a = 0.561$, $b = 1.190$ and $c = 0.042$, $d = b + c$, e = d and $f = e$.

computed with the PZ2 (paramagnetic zero) variant[18] of the CTOCD method. As expected from the near invariance of the current density maps between planar and non-planar forms, the mean shieldings, σ(av), of corresponding rings are almost identical in **2a**, **b** and again in **3a**–**c**. Planarity is not a major determinant of the average shielding here. However, the near constancy of the average in-plane values σ(in) across all rings in **1**, **2a** and **3a** implies that the mean values, and hence the NICS values[12] obtained from them by change of sign, are in fact less useful as indicators of local circulation than the out-of-plane component σ(out), particularly when bifurcation of current is present,[28] as in ring ***D*** in **1**, or when currents alternate around a ring, as in ***B*** in **3a**–**c**. Reference to the total current density maps of Figure 1 shows that there is a precise correspondence of σ(out) with the sense of rotation in the central ring ***A***: a positive out-of-plane component is found for a diamagnetic (anti-clockwise) circulation of electrons, a negative component for paramagnetic (clockwise) circulation. For **1** and **2**, Clar circulations on the neighbouring hexagons contribute to the paramagnetism of ring ***B***, but the alternately opposed σ and π current densities in the bonds of ***B*** lead to a near-zero value of σ(out) for this ring in **3a**. The positive values of σ(out) for ring ***C*** in **1** and **2** reflect the diamagnetic nature of the Clar circulation. Ring ***D*** is clearly diamagnetic in **3a**–**c**, but has bifurcated flow in **1**, which is reflected in a small value of σ(out) in that case. The corresponding NICS [≡ −σ(av)] values for the various rings in these widely different magnetic environments are less informative.

The deshielding effects of the giant π currents around the perimeter are demonstrated by the computed ^{1}H NMR shifts. In Table 3 are shown components of the computed ^{1}H absolute shielding tensors and δ values for the distinct boundary hydrogens in the three molecules (Scheme 1). Also shown for the planar structures are estimates of the maximum magnitudes, j_{max}, of the π current on the neighbouring carbon atoms (evaluated in the plotting plane and given in units of that computed in benzene). The out-of-plane component σ(out) directly reflects the influence of the local field from the induced current density, and is the principal contributor to the trend in the observable, the ^{1}H NMR chemical shift δ.

Table 3. ^{1}H Magnetic shielding tensors and related quantities for **1**, **2a**, **b** and **3a**–**c**: j_{max} is the maximum magnitude of the π current density at 1 a_0 above the bonded carbon. σ(out), σ(in) and σ(av) (in ppm) are the out-of-plane component, the mean in-plane component and the mean, respectively. δ is the chemical shift derived from the computed shielding as $\delta = 30.8 - \sigma(av) \times 10^6$ [ppm].[25] For the non-planar compounds **2b** and **3b**–**c**, only the *isotropic* σ(av) values are shown.

Compound[a]	Hydrogen[a]	j_{max}	σ(out)	σ(in)	σ(av)	δ
1 (D_{6h})	H*1*	2.0	7.0	26.9	20.2	10.6
	H*2*	1.1	10.8	26.3	21.1	9.7
2a (D_{6h})	H*1*	1.2	16.8	25.4	22.6	8.2
	H*3*	1.2	12.8	26.8	22.1	8.7
2b (D_{3d})	H*1*				22.7	8.1
	H*3*				22.1	8.7
3a (D_{6h})	H*2*	1.1	17.8	25.6	23.0	7.8
	H*4*	1.1	4.3	28.0	20.1	10.7
3b (D_6)	H*2*				23.1	7.7
	H*4*				21.9	8.9
3c (D_{3d})	H*2*				23.0	7.8
	H*4*				21.1	9.7

[a] See Scheme 1.

The two boundary hydrogens (H*1* and H*2*) in **1** show a significant deshielding; compared to the corresponding ^{1}H NMR chemical shifts for anthracene [σ(av); H*1* 22.8 ppm (δ= 8.0) and H*2* 23.2 (δ = 7.6) ppm] calculated in the same approach, each is deshielded by over 2 ppm, with the greater effect at site H*1* of **1**, where j_{max} is at its largest. In the case of **2a** and **2b** the two boundary hydrogens (H*1* and H*3*) can be compared to those in either phenanthrene [σ(av); H*1* 23.3 ppm (δ = 7.5) and H*3* 22.7 (δ = 8.1) ppm] or triphenylene [σ(av); H*1* 23.3 ppm (δ = 7.5) and H*3* 22.8 (δ = 8.0) ppm]. For **3** the natural comparison is with non-planar benz[*c*]phenanthrene [σ(av); H*2* 23.5 ppm (δ 7.3) and H*4* 22.0 (δ = 8.8) ppm]; whereas H*2* is lightly deshielded by the perimeter current the high δ value of H*4* in **3a** (10.7 ppm) reflects the steric strain at this site which drops significantly in the non-planar structures **3b, c**.

Conclusion

The current densities induced in three large alternating polycyclic molecules all with apparently similar sixfold structures have been visualised by using an ipsocentric ab initio method. The maps show that **1**–**3** support distinctly different ring current patterns, which maintain their form even where the minimum-energy structure is non-planar. All three molecules show a strong diatropic current that takes the shape of the carbon perimeter, in **1** and **2** subsuming local Clar sextet benzenoid currents, but in **3** forming a single monocyclic circuit on 42 carbon atoms. The central hexagon behaves as a magnetically isolated unit, in **1** and **2** supporting a conventional benzenoid diatropic current, but in **3** the counter-circulating paratropic current characteristic of an [*n*]circulene.[25] These differences can be rationalised in terms of orbital contributions dominated by the electrons in the frontier orbitals.

Perimeter topology is evidently exercising a controlling influence on the current pattern and can be expected to be a major factor in designing π-conjugated molecules for materials applications that depend on electron mobility. The relationship between magnetic properties, boundary shape and molecular size for circumscribed polycyclic aromatic hydrocarbons will be the subject of future investigation.

Acknowledgement

We acknowledge a travel grant from the Royal Society of Chemistry (International Travel Grant 0012289; L.W.J.) and financial support from the European Union TMR and Marie Curie schemes, contracts FMRX-CT097-0192 (BIOFULLERENES, R.W.A.H.) and HPMT-CT-2000-00016 (A.S.).

[1] For a recent review: U. E. Wiersum, L. W. Jenneskens in *Gas Phase Reactions in Organic Synthesis*, (Ed.: Y. Vallée), Gordon and Breach Science Publishers, Amsterdam, The Netherlands, **1997**, pp. 143—194, and references therein.
[2] For a recent review: A. J. Berresheim, M. Müller, K. Müllen, *Chem. Rev.* **1999**, *99*, 1747—1785, and references therein.
[3] C. W. Bauschlicher, Jr, E. L. O. Bakes, *Chem. Phys.* **2000**, *262*, 285–291, and references therein.
[4] For example: A. M. Craats, J. M. Warman, K. Müllen, Y. Geerts, J. D. Brand, *Adv. Mater.* **1998**, *10*, 36–38, and references therein.
[5] F. Morgenroth, C. Kübel, M. Müller, U. M. Wiesler, A. J. Berresheim, M. Wagner, K. Müllen, *Carbon* **1998**, *36*, 833–837; F. Dötz, J. D. Brand, S. Ito, L. Ghergel, K. Müllen, *J. Am. Chem. Soc.* **2000**, *122*, 7707–7717, and references therein.
[6] K. Yoshimura, L. Przybilla, S. Ito, J. D. Brand, M. Wehmeir, H. J. Räder, K. Müllen, *Macromol. Chem. Phys.* **2001**, *202*, 215–222, and references therein.
[7] S. E. Stein, R. L. Brown, *J. Am. Chem. Soc.* **1987**, *109*, 3721–3729; F. Dietz, N. Tyutyulkov, G. Madjarova, K. Müllen, *J. Phys. Chem. B* **2000**, *104*, 1746–1761.
[8] T. A. Keith, R. F. W. Bader, *Chem. Phys. Lett.* **1993**, *210*, 223–231; S. Coriani, P. Lazzeretti, M. Malagoli, R. Zanasi, *Theor. Chim. Acta* **1994**, *89*, 181–192.
[9] W. Hendel, Z. H. Kahn, W. Schmidt, *Tetrahedron* **1986**, *42*, 1127–1134.
[10] E. Clar, J. F. Stephen, *Tetrahedron* **1965**, *21*, 467–470; E. Clar, W. Schmidt, W. *Tetrahedron* **1977**, *33*, 2093–2097.
[11] N. Trinajstić, *Chemical Graph Theory*, *Second Edition*, CRC Press: Baco Raton, USA, **1992**, Chapter 8.
[12] P. von R. Schleyer, C. Maerker, A. Dransfeld, H. Jiao, H.; N. J. R. van Eikema Hommes, *J. Am. Chem. Soc.* **1996**, *118*, 6137–6138.
[13] R. D. Amos, J. E. Rice, *The Cambridge Analytical Derivatives Package*, *Issue 4.0*, 1987.
[14] GAUSSIAN98 (Revision A.9), M. J. Frisch, G. W. Trucks, H. B. Schlegel, G. E. Scuseria, M. A. Robb, J. R. Cheeseman, V. G. Zakrzewski, J. A. Montgomery, R. E. Stratmann, J. C. Burant, S. Dapprich, J. M. Millam, A. D. Daniels, K. N. Kudin, M. C. Starin, O Farkas, J. Tomasi, V. Barone, M. Cossi, R. Cammi, B. Mennucci, C. Pornelli, C.

Adamo, S. Clifford, J. Ochterski, G. A. Petersson, P. Y. Ayala, Q. Cui, K. Morokuma, D. K. Malick, A. D. Rabuck, K. Raghavachari, J. B. Foresman, J. Cioslowski, J. V. Ortiz, B. B. Stefanov, G. Liu, A. Liashenko, P. Piskorz, I. Komaromi, R. Gomperts, R. L. Martin, D. J. Fox, T. Keith, M. A. Al-Laham, C. Y. Peng, A. Nanayakkara, C. Gonzalez, M. Challacombe, P. M. W. Gill, B. G. Johnson, W. Chen, M. W. Wong, J. L. Andres, M. Head-Gordon, E. S. Replogle, J. A. Pople, *Gaussian*, *Inc:* Pittsburg PA, **1998**.

[15] P. Lazzeretti, R. Zanasi, R. *SYSMO Package*; University of Modena: Modena, Italy, 1980, with additional routines for evaluation and plotting of current density by E. Steiner and P. W. Fowler.

[16] E. Steiner, P. W. Fowler, *Int. J. Quant. Chem.*, **1996**, *60*, 609–616.

[17] E. Steiner, P. W. Fowler, *J. Phys. Chem. A* **2001**, *105*, 9553–9562.

[18] R. Zanasi, P. Lazzeretti, M. Malagoli, F. Piccinini, F. *J. Chem. Phys.* **1995**, *102*, 7150–7157.

[19] R. Zanasi, *J. Chem. Phys.* **1996**, *105*, 1460–1469.

[20] F. L. Hirshfeld, S. Sandler, G. M. Schmidt, *J. Chem. Soc.* **1963**, 2108–2125.

[21] R. Goddard, M. W. Haenel, W. C. Herndon, C. Kruger, M. Zander, *J. Am. Chem. Soc.* **1995**, *117*, 30–41.

[22] A. Soncini, P. W. Fowler, I. Černušak, E. Steiner, *Phys. Chem. Chem. Phys.* **2001**, *3*, 3920–3923.

[23] E. Clar, *Polycyclic Hydrocarbons*, Academic Press Inc., London, **1964**.

[24] P. Lazzeretti, *Prog. Nucl. Magn. Res.* **2000**, *36*, 1–8, and references therein.

[25] E. Steiner, P. W. Fowler, L. W. Jenneskens, *Angew. Chem.* **2001**, *113*, 375—379; *Angew. Chem. Int. Ed.* **2001**, *40*, 362—366, and references therein.

[26] E. Steiner, P. W. Fowler, *Chem. Commun.* **2001**, 2220–2221.

[27] A. Pasquarello, M. Schlüter, R. C. Haddon, *Phys. Rev. A* **1993**, *47*, 1783–1789.

[28] E. Steiner, P. W. Fowler, *ChemPhysChem.* **2002**, *1*, 114–116.

Received: June 17, 2002 [F4183]

